Finite Element and Subspace Identification Approaches to Model Development of a Smart Acoustic Box with Experimental Verification

Tamara Nestorović, Jean Lefèvre, Stefan Ringwelski, and Ulrich Gabbert

***Abstract*—**Two approaches for model development of a smart acoustic box are suggested in this paper: the finite element (FE) approach and the subspace identification. Both approaches result in a state-space model, which can be used for obtaining the frequency responses and for the controller design. In order to validate the developed FE model and to perform the subspace identification, an experimental set-up with the acoustic box and dSPACE system was used. Experimentally obtained frequency responses show good agreement with the frequency responses obtained from the FE model and from the identified model.

***Keywords*—**Acoustic box, experimental verification, finite element model, subspace identification.

I. Introduction

ENGINEERING of smart structures gains more and more interest in the recent years due to their characteristics of adaptation to changing environmental and working conditions owing to integrated active materials used as actuators and sensors and implemented control. Development of reliable models of active structures is therefore of interest especially in the early design stages, since it enables development and testing of different control techniques and investigation of the structural behavior under different simulated conditions.

In this paper a smart acoustic box is considered and for its modeling two approaches are suggested: numerical modeling based on the finite element method (FEM) and experimental subspace identification.

The FEM approach takes into consideration the electro-mechanical-acoustic effects. After appropriate transformations and modal reduction, FEM based state-space model is obtained, which can be used to study different effects. Reduced order state-space models are also convenient from the controller design point of view.

Experimental identification using the subspace-based algorithm is suggested as another modeling option, which also results in a state-space model. It enables a successful modeling of multiple-input multiple-output (MIMO) systems based on the measurement of the input and output signals.

Theoretical backgrounds of both approaches are presented in this paper and verified on the example of modeling a smart acoustic box with attached piezoelectric patches used as actuators and sensors. As a result different frequency response functions obtained on the basis of developed models are shown. Comparison between the model based frequency responses and the measured ones shows a good agreement, which confirms the feasibility of the suggested modeling techniques.

II. Finite Element Formulation

Engineering of smart structures with distributed piezoelectric patches used as actuators and sensors requires adequate numerical simulation tools, which enable development of overall smart structure models including mechanical, electrical and acoustic effects. For the simulation of coupled electro-mechanical-acoustical problems regarding interior noise, a FEM based approach proposed by the authors [1]–[3] can be used.

Modeling and simulation of the coupled electro-mechanical-acoustical problems using the FEM approach is performed using the general purpose FEM software package COSAR [4], which contains an extensive library of multi-field finite elements for 1D, 2D and 3D continua as well as for shell-type thin walled structures and acoustic brick-type elements in order to simulate piezoelectrically controlled vibro-acoustic systems. Considering small displacements and regarding acoustic responses as small perturbations to an ambient reference state, the derivation of the finite element model is based on the mechanical equilibrium, the electric equilibrium, the linear coupled electromechanical constitutive equations and the linear acoustic wave equation [1].

Following the standard FEM procedure described in detail in [3] the semi discrete system of coupled equations of the electromechanical field and the acoustic field is obtained in

Manuscript received January 25, 2007. This work was supported by the German Research Foundation (DFG) in the frame of the research project NE 1372/2-1. This support is gratefully acknowledged.

Dr.-Ing. T. Nestorović is with the Institute of Mechanics, Otto-von-Guericke University Magdeburg, Universitätsplatz 2, D-39106 Magdeburg, Germany (phone: +49-391-6711724; fax: +49-391-6712439; e-mail: tamara.nestorovic@ mb.uni-magdeburg.de).

Dipl.-Ing. J. Lefèvre was with Otto-von-Guericke University Magdeburg, Universitätsplatz 2, D-39106 Magdeburg, Germany. He is now with the FEMCOS - Ingenieurbüro mbH, Herrenkrugstraße 9, D-39114 Magdeburg, Germany (e-mail: jean.lefevre@femcos.de).

Prof. Dr.-Ing. habil. U. Gabbert and Dipl.-Ing. Stefan Ringwelski are with the Institute of Mechanics, Otto-von-Guericke University Magdeburg, Universitätsplatz 2, D-39106 Magdeburg, Germany (e-mail: ulrich.gabbert@ mb.uni-magdeburg.de, stefan.ringwelski@ mb.uni-magdeburg.de).

the form of the following matrix equation:

$$\begin{bmatrix} \mathbf{M}_{ww} & \mathbf{0} & \mathbf{0} \\ \mathbf{0} & \mathbf{0} & \mathbf{0} \\ \mathbf{0} & \mathbf{0} & -\rho_0 \mathbf{M}_a \end{bmatrix} \begin{bmatrix} \ddot{\mathbf{w}} \\ \ddot{\boldsymbol{\varphi}} \\ \ddot{\boldsymbol{\Phi}} \end{bmatrix} + \begin{bmatrix} \mathbf{C}_{ww} & \mathbf{0} & -\mathbf{C}_{wc} \\ \mathbf{0} & \mathbf{0} & \mathbf{0} \\ -\mathbf{C}_{wc}^T & \mathbf{0} & -\rho_0 \mathbf{C}_a \end{bmatrix} \begin{bmatrix} \dot{\mathbf{w}} \\ \dot{\boldsymbol{\varphi}} \\ \dot{\boldsymbol{\Phi}} \end{bmatrix} + \begin{bmatrix} \mathbf{K}_{ww} & \mathbf{K}_{w\varphi} & \mathbf{0} \\ \mathbf{K}_{w\varphi}^T & -\mathbf{K}_{\varphi\varphi} & \mathbf{0} \\ \mathbf{0} & \mathbf{0} & -\rho_0 \mathbf{K}_a \end{bmatrix} \begin{bmatrix} \mathbf{w} \\ \boldsymbol{\varphi} \\ \boldsymbol{\Phi} \end{bmatrix} = \begin{bmatrix} \mathbf{f}_{ww} \\ \mathbf{f}_{\varphi} \\ -\rho_0 \mathbf{f}_a \end{bmatrix} \tag{1}$$

with mass matrix $\mathbf{M}_{ww}$, proportional damping matrix $\mathbf{C}_{ww}$, stiffness matrix $\mathbf{K}_{ww}$, electric matrix $\mathbf{K}_{\varphi\varphi}$, piezoelectric coupling matrix $\mathbf{K}_{w\varphi}$, mechanical load vector $\mathbf{f}_{ww}$ and electric load vector $\mathbf{f}_{\varphi}$. The quantities regarding the acoustic field are: constant fluid density ρ_0, acoustic mass matrix $\mathbf{M}_a$, acoustic damping matrix $\mathbf{C}_a$, acoustic stiffness matrix $\mathbf{K}_a$ and the acoustic load vector due to prescribed normal velocities $\mathbf{f}_a$. Vibro-acoustic coupling is performed in terms of the coupling matrix $\mathbf{C}_{wc}$ arising from an additional load, which acts on the fluid-structure interface and originates from the sound pressure for the structure and from the normal velocity of the structure for the acoustic fluid. Vector $\mathbf{w}$ contains all nodal mechanical degrees of freedom, $\boldsymbol{\varphi}$ is the vector of nodal electric potentials and $\boldsymbol{\Phi}$ the fluid velocity potential vector.

The aim of the overall model development is to obtain a suitable basis for further investigations on possibilities for the vibration and noise reduction using control techniques. This aim requires on one hand a model in an appropriate form (e.g. the state-space form, which is convenient for the controller design purposes), but on the other hand also a model which offers suitable numerical performance of the calculation, which in turn enables subsequent real-time controller implementation. The finite element model based on (1) contains a large number of degrees of freedom. Modal truncation based on a reduced number of preselected uncoupled eigenmodes represents a common model reduction technique, which provides a model with the previously stated performances. After a sequence of mathematical transformations (for more details see [2], [3]) the modal truncation results in a state equation (2) of the standard state-space model used in the control theory. The state-space model is completed with the output (measurement) equation (3).

$$\dot{\mathbf{x}}(t) = \mathbf{A}\mathbf{x}(t) + \mathbf{B}\mathbf{u}(t) + \mathbf{E}\mathbf{f}(t) \tag{2}$$

$$\mathbf{y}(t) = \mathbf{C}\mathbf{x}(t) + \mathbf{D}\mathbf{u}(t) + \mathbf{F}\mathbf{f}(t) \tag{3}$$

Vector $\mathbf{x}$ is the vector of modal coordinates (such that $\mathbf{z} = \mathbf{Q}\mathbf{x}$) obtained through the ortho-normalization, where $\mathbf{Q}$ represents the modal matrix obtained as a solution of the eigenvalue problem of the homogeneous part of the equation (1) with the introduced state-space vector:

$$\mathbf{z} = \left[\mathbf{w} \quad \boldsymbol{\varphi} \quad \boldsymbol{\Phi} \quad \dot{\mathbf{w}} \quad \dot{\boldsymbol{\varphi}} \quad \dot{\boldsymbol{\Phi}}\right]. \tag{4}$$

Notations in (2) and (3) have the following meanings: $\mathbf{A}$ denotes the state matrix, $\mathbf{B}$ is the control input matrix, $\mathbf{E}$ is the disturbance coupling matrix, $\mathbf{C}$ output matrix, $\mathbf{D}$ input-to-output coupling matrix and $\mathbf{F}$ disturbance-to-output coupling matrix. Vector $\mathbf{f}(t)$ represents the vector of external disturbances, $\mathbf{u}(t)$ is the vector of the controller influence and $\mathbf{y}(t)$ the output (measurement) vector.

Verification of the presented FEM based modeling and simulation approach is performed in the subsequent sections through the model identification in the state-space form and through experimental investigations.

III. Subspace Identification

In this paper the subspace identification [5]–[10] is used to obtain experimentally the model of the piezoelectric mechanical structure influenced by the surrounding acoustic fluid in the state-space form. The method of the identification is general – it applies to a wide range of model identification problems, where based on the measured input and output signals a state-space model is to be determined. The experimental investigations described in this paper are aimed at verification of the suggested FEM based modeling on one hand, and on the other hand at obtaining the experimental model in the comparable state-space form in order to draw out the conclusions regarding the reliability of the models obtained using both modeling methods as well as regarding the minimal model orders which meet the required performances of the frequency responses.

Since the subspace identification is based on sampled input/output measurement signals, the method applies to a discrete-time form of the resulting state-space model. Using the subspace identification, the model can be identified in a general deterministic-stochastic form of a discrete-time state-space equivalent of the model (2), (3):

$$\begin{aligned} \mathbf{x}[k+1] &= \boldsymbol{\Phi}\mathbf{x}[k] + \boldsymbol{\Gamma}\mathbf{u}[k] + \boldsymbol{w}[k] \\ \mathbf{y}[k] &= \mathbf{C}\mathbf{x}[k] + \mathbf{D}\mathbf{u}[k] + \boldsymbol{v}[k] \end{aligned} \tag{5}$$

with discrete-time state and control matrices $\boldsymbol{\Phi}$ and $\boldsymbol{\Gamma}$, and the process and the measurement noise $\boldsymbol{w}[k]$ and $\boldsymbol{v}[k]$, respectively. The process noise and the measurement noise vector sequences $\boldsymbol{w}[k]$ and $\boldsymbol{v}[k]$ are white noise with zero mean and with covariance matrix:

$$\mathcal{E}\left\{\begin{bmatrix} \boldsymbol{w}[i] \\ \boldsymbol{v}[j] \end{bmatrix} \begin{bmatrix} \boldsymbol{w}[i]^{\mathrm{T}} & \boldsymbol{v}[j]^{\mathrm{T}} \end{bmatrix}\right\} = \begin{bmatrix} \mathbf{Q} & \mathbf{S} \\ \mathbf{S}^{\mathrm{T}} & \mathbf{R} \end{bmatrix} \tag{6}$$

The general deterministic-stochastic problem of the subspace identification is to determine the order n of the unknown system and the system matrices $\boldsymbol{\Phi} \in \mathrm{R}^{n\times n}$, $\boldsymbol{\Gamma} \in \mathrm{R}^{n\times m}$, $\mathbf{C} \in \mathrm{R}^{l\times n}$, $\mathbf{D} \in \mathrm{R}^{l\times m}$ as well as the covariance matrices $\mathbf{Q} \in \mathrm{R}^{n\times n}$, $\mathbf{S} \in \mathrm{R}^{n\times l}$, $\mathbf{R} \in \mathrm{R}^{l\times l}$ of the noise sequences $\boldsymbol{w}[k]$ and $\boldsymbol{v}[k]$. Subsequent derivations regard the pure deterministic case considered in [11].

Measured input and output data are organized into block Hankel matrices defined in the following form [5]:

$$\mathbf{U} = U_{0|2i-1} = \left[\begin{array}{ccccc} \mathbf{u}_0 & \mathbf{u}_1 & \mathbf{u}_2 & \cdots & \mathbf{u}_{j-1} \\ \mathbf{u}_1 & \mathbf{u}_2 & \mathbf{u}_3 & \cdots & \mathbf{u}_j \\ \cdots & \cdots & \cdots & \cdots & \cdots \\ \mathbf{u}_{i-1} & \mathbf{u}_i & \mathbf{u}_{i+1} & \cdots & \mathbf{u}_{i+j-2} \\ \hline \mathbf{u}_i & \mathbf{u}_{i+1} & \mathbf{u}_{i+2} & \cdots & \mathbf{u}_{i+j-1} \\ \mathbf{u}_{i+1} & \mathbf{u}_{i+2} & \mathbf{u}_{i+3} & \cdots & \mathbf{u}_{i+j} \\ \cdots & \cdots & \cdots & \cdots & \cdots \\ \mathbf{u}_{2i-1} & \mathbf{u}_{2i} & \mathbf{u}_{2i+1} & \cdots & \mathbf{u}_{2i+j-2} \end{array}\right]. \quad (7)$$

The output block Hankel matrix $Y_{0|2i-1}$ is defined in a similar way. For more details on definition of the Hankel matrices and the subspace-based identification method see [5], [9]–[11]. The measurement data are organized in the form of the input-output relation [5]:

$$\mathbf{Y}[k] = \mathbf{\Gamma}_\alpha \mathbf{x}[k] + \mathbf{\Phi}_\alpha \mathbf{U}[k] \quad (8)$$

where $\mathbf{\Gamma}_\alpha$ represents the observability matrix for the system (5), $\mathbf{\Phi}_\alpha$ is the Toeplitz matrix [6] of impulse responses from **u** to **y**:

$$\mathbf{\Phi}_\alpha = \begin{bmatrix} \mathbf{D} & 0 & \cdots & \mathbf{0} \\ \mathbf{C\Gamma} & \mathbf{D} & & \mathbf{0} \\ \vdots & \ddots & \ddots & \vdots \\ \mathbf{C\Phi}^{\alpha-2}\mathbf{\Gamma} & \cdots & \mathbf{C\Gamma} & \mathbf{D} \end{bmatrix} \quad (9)$$

and α is a specified number greater than the state dimension but much smaller than the data length. For a deterministic case [7], [11] the problem is simplified to determining $\mathbf{\Gamma}_\alpha$ and $\mathbf{\Phi}_\alpha$ by computing the singular value decomposition (SVD) of **U** in the first step:

$$\mathbf{U} = \mathbf{P\Sigma Q}^{\mathrm{T}} = [\mathbf{P}_{u1} \quad \mathbf{P}_{u2}] \begin{bmatrix} \mathbf{\Sigma}_u & 0 \end{bmatrix} \begin{bmatrix} \mathbf{Q}_{u1}^{\mathrm{T}} \\ \mathbf{Q}_{u2}^{\mathrm{T}} \end{bmatrix}. \quad (10)$$

If matrix **U** has dimension $m \times n$ and rank r, then the partition in (10) is performed as follows:

$$\mathbf{P} = [\mathbf{p}_1 \quad \cdots \quad \mathbf{p}_r \mid \mathbf{p}_{r+1} \quad \cdots \quad \mathbf{p}_m] = [\mathbf{P}_{u1} \quad \mathbf{P}_{u2}] \quad (11)$$

$$\mathbf{Q} = [\mathbf{q}_1 \quad \cdots \quad \mathbf{q}_r \mid \mathbf{q}_{r+1} \quad \cdots \quad \mathbf{q}_n] = [\mathbf{Q}_{u1} \quad \mathbf{Q}_{u2}] \quad (12)$$

where $\mathbf{p}_i$ are the left singular vectors of **U** [12]. It can be shown that they are eigenvectors of $\mathbf{UU}^{\mathrm{T}}$. Vectors $\mathbf{q}_i$ are the right singular vectors of **U**. It can be shown that they are eigenvectors of $\mathbf{U}^{\mathrm{T}}\mathbf{U}$. Multiplying (8) by $\mathbf{Q}_{u2}$, matrix $\mathbf{\Gamma}_\alpha$ can be determined from a SVD of $\mathbf{YQ}_{u2}$. Then matrix **C** is obtained as the first row (in a sense of a block-row) of the observability matrix $\mathbf{\Gamma}_\alpha$, and matrix $\mathbf{\Phi}$ is calculated from: $\underline{\mathbf{\Gamma}}_\alpha = \overline{\mathbf{\Gamma}}_\alpha \mathbf{\Phi}$ applying pseudo inverse, where $\overline{\mathbf{\Gamma}}_\alpha$ is obtained by dropping the last row of $\mathbf{\Gamma}_\alpha$. Matrix $\underline{\mathbf{\Gamma}}_\alpha$ represents the matrix obtained by dropping the first row of $\mathbf{\Gamma}_\alpha$. For the calculation of $\mathbf{\Gamma}$ and **D** matrices, (8) is multiplied by the pseudo inverse of **U** on the right and by $\mathbf{P}_{u2}^{\mathrm{T}}$ from (10) on the left. Thus the equation is reduced to:

$$\mathbf{P}_{u2}^{\mathrm{T}} \mathbf{Y} \mathbf{U}^{-1} = \mathbf{P}_{u2}^{\mathrm{T}} \mathbf{\Phi}_\alpha . \quad (13)$$

After rearranging, (13) can be solved for $\mathbf{\Gamma}$ and **D** using the least squares, see (9). In this way the system parameters in the form of state-space matrices of the model (5) are identified using the subspace-based identification method.

IV. Experimental Rig with the Acoustic Box

Described procedures for the FEM modeling and subspace identification were implemented and tested using the experimental set-up with the smart plate with piezoelectric patches and the acoustic box with the air as acoustic fluid within it. The aim of the experiment is verification of the FEM modeling procedure [13] and identification of the state-space model using the subspace method and its comparison with the numerically developed FEM based state-space model.

The acoustic box set-up consists of a clamped aluminium plate with fifteen piezoelectric patches attached to its inner surface (Fig. 1) and of the wooden box comprising the acoustic fluid – air. The side of the box opposite to the aluminium plate is open. The acoustic box with the dimensions used for the numerical modeling is represented in Fig. 2.

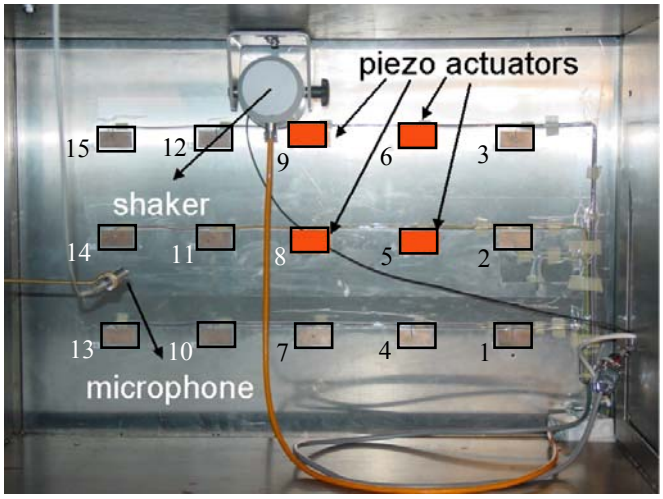

Fig. 1 Inner side of the plate with attached piezo patches

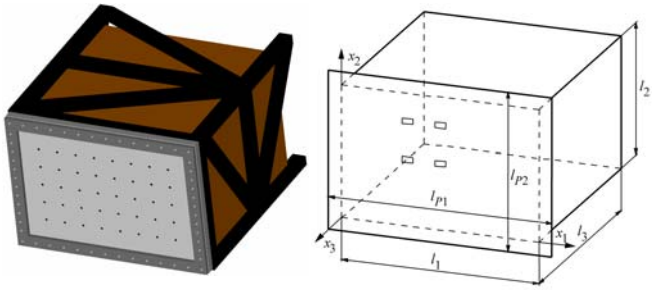

Fig. 2 Acoustic box with dimensions

Dimensions of the plate are: l_{P1} = 1020 mm, l_{P2} = 720 mm, h = 4 mm, dimensions of the cavity: l_1 = 900 mm, l_2 = 600 mm,
l_3 = 1250 mm, dimensions of the patches: 50 mm × 25 mm × 0.2 mm.

The plate is excited using a shaker driven by computer

generated random noise signals. The impedance head placed on the top of the rig connected to the shaker measures the shaker force signal. The sound pressure at the predefined point of the acoustic box (x_1 = 650 mm, x_2 = 300 mm, x_3 = 525 mm) is measured using a microphone. Acoustic box is placed in the sound low-reflection room in order to eliminate environmental influences during the measurements. The scheme of the experimental rig with all included measurement devices for experimental determining of the frequency responses (experimental verification of the FEM model) and for the experimental subspace-based model identification is shown in Fig. 3.

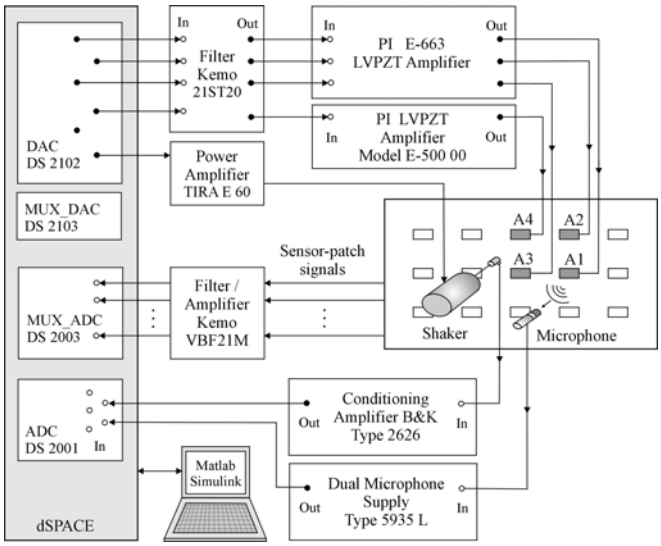

Fig. 3 Experimental rig for the frequency response determining and the state-space model identification

Excitation signals for the shaker are generated by the computer linked to the dSPACE system with ADC and DAC boards shown in Fig. 3. Random noise excitation signal from the DAC board DS 2102 (range ±5V) of the dSPACE system is amplified by the Power Amplifier TIRA E 60 and led to the shaker. Excitation force exerted by the shaker is measured using the force gauge Impedance Head B&K Type 8001, the signal of which is fed to the dSPACE ADC board DS 2001 (range ±5V) via the Conditioning Amplifier B&K Type 2626, which calibrates the force signal. The conditioning amplifier outputs 0.1 V per measured unit, in this case per electric charge produced by the impedance head of the sensitivity 369 pC/N, which is also set on the conditioning amplifier. Therefore the output of the conditioning amplifier of 0.1V corresponds to the shaker force of 1N. The frequency range set on the conditioning amplifier is between 1 Hz and 1 kHz.

Another signal acquired by the ADC board DS 2001 of the dSPACE system is the air pressure signal on the microphone. The microphone signal is amplified with the gain 10 dB through the Dual Microphone Supply Type 5935 L. The sensitivity of the microphone is 50.8 mV/Pa.

Selected piezo patches are used as sensors. Their voltage signals are filtered in the predefined frequency range of 1 kHz and amplified with the gain of 12 dB through the Filter/Amplifier Kemo VBF21M. Signal acquisition of the sensor-patches is performed on the MUX_ADC board DS 2003 (range ±5V) of the dSPACE system using the input channels of this board.

For the identification of the MIMO models of the acoustic box the measurement of the excitation signals from the selected actuator-patches is required. The piezo patches numerated as 5, 6, 8 and 9 (Fig. 1) were selected as actuators for the purpose of numerical FEM modeling. For the sake of the consistency between the numeric and experimental (identified) model, the same patches 5, 6, 8, 9 are used respectively as actuators A1, A2, A3, A4 during the data acquisition for the model verification and identification purposes. Random noise signals generated by the computer are output through the DAC board DS2102 (range ±5V) of the dSPACE. They are first filtered through the low-pass filter Kemo 21ST20 with the cut-off frequency of 1 kHz and afterwards amplified through the piezo amplifiers PI E-663 LVPZT (for the first three channels/actuators) and PI LVPZT Model E-500 00 (for the fourth channel/actuator) with the gain 10 and offset 50V. For the controller implementation purposes the actuator signals of the predefined controller can be fed to the piezo actuators in the similar way.

V. Experimental Results

Using described experimental set-up the verification of the numerical FEM model and the subspace identification were performed.

A. Experimental Frequency Responses and Comparison with FEM Results

The frequency responses of the acoustic box are determined experimentally and on the basis of the numerical FEM model. Calculated eigenfrequencies of the modally truncated FEM based state-space model for the first five structural (index *w*) and acoustic modes (index *a*) are listed in the Table I.

TABLE I
Calculated Eigenfrequencies of the Elastic Plate and of the Acoustic Cavity

Number *i*	1	2	3	4	5
f_{wi} [Hz]	66.7	106.2	163.8	172.1	201.2
ω_{wi} [rad/s]	419.1	667.3	1029.2	1081.3	1264.2
f_{ai} [Hz]	68.0	200.8	204.0	278.1	291.5
ω_{ai} [rad/s]	427.3	1261.7	1281.8	1747.4	1831.6

Experimental frequency response functions (FRFs) were determined based on the selected measured input and output signals, i.e. their fast Fourier transforms (FFTs). The FRF expresses a frequency domain relationship (in terms of ratio) between a response signal (output) and a reference signal (input) of a linear time-invariant system, i.e. the ratio of their FFTs. For three different sensor-patch constellations (Table II) all combinations of the output-to-input FRFs were determined

(actuator-to-sensor, shaker-to-sensor, actuator-to-microphone, sensor-to-microphone) and compared with the corresponding frequency responses determined on the basis of the numerically obtained state-space model of the order 20. In the numerical state-space model as well as for its experimental verification and subspace identification the actuator-patch signals were considered as inputs, the shaker force signal as measurable disturbance input, and the sensor-patch and microphone signals as the measured outputs. For all three actuator/sensor constellations the patches 5, 6, 8, 9 were used as actuators (consistency with the numerical model, as previously stated). Sensor groups for the three constellations are shown in Table II.

TABLE II
PIEZO PATCHES OF THE THREE SENSOR CONSTELLATIONS

	Constellation 1	Constellation 2	Constellation 3
Sensor 1	2	3	4
Sensor 2	4	7	7
Sensor 3	7	11	10
Sensor 4	11	12	11

Selected frequency responses are represented in the following figures showing a good agreement between the experimental and numerical results.

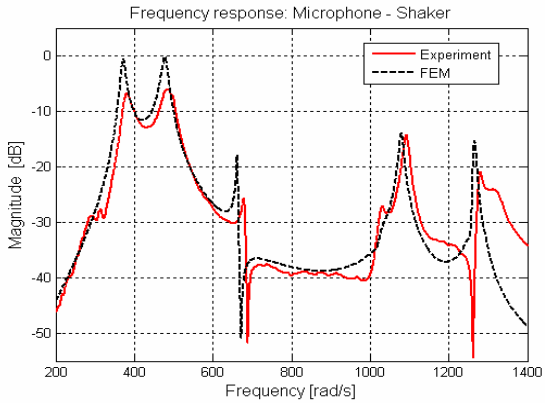

Fig. 4 Excitation by shaker (valid for all three sensor constellations)

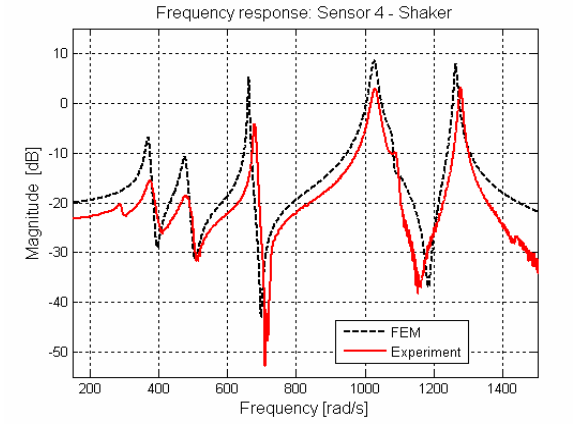

Fig. 5 Excitation by shaker (constellation 2)

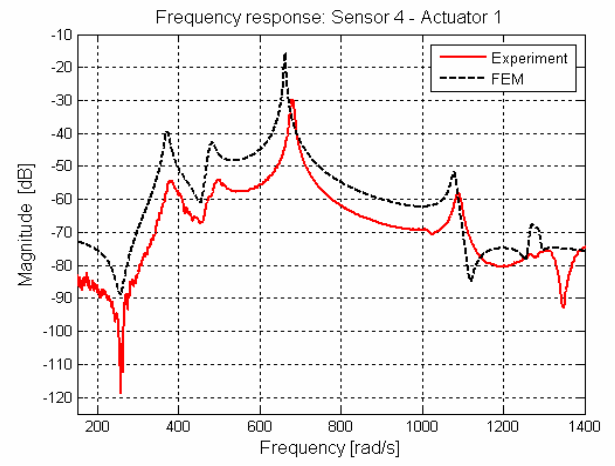

Fig. 6 Excitation by actuator-patch (constellation 3)

Figs 4 – 6 show the comparison of the experimental and numerical results for the single-input single-output (SISO) case when the acoustic plate is excited only by a shaker or only by a single actuator-patch and the signals are measured on the microphone or on the appropriate sensor-patches.

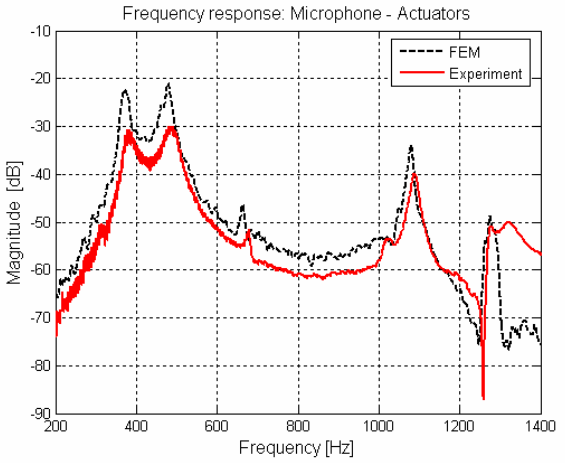

Fig. 7 Excitation by shaker and actuator-patches (constellation 1– MIMO case)

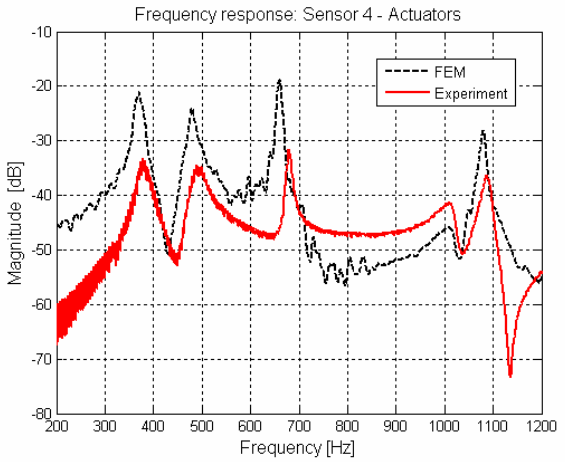

Fig. 8 Excitation by shaker and actuator-patches (constellation 1 – MIMO case)

For the investigation of MIMO models the responses of the sensor-patches were acquired under excitation by four actuator-patches and by the shaker. Selected frequency responses obtained experimentally and on the basis of the reduced FEM model are compared in the Figs. 7 and 8. First the experimental FRFs (solid line) were obtained under random excitation by shaker and actuator-patches. During the experiment the excitation signals were acquired and saved using dSPACE. The same excitations were used for the simulation with the reduced FEM based state-space model and based on the obtained simulated time responses, using the FFTs, the FEM based FRFs were obtained (dashed black line).

B. Experimental Subspace Identification

The MIMO model subspace identification of the acoustic box was performed on the basis of the measured input/output signals using the experimental rig shown in Fig. 3 and applying the identification algorithm (described in section III) and the auxiliary Matlab function *n4sid* [14]. The criterion for selection of the model order was to obtain a MIMO state-space model, from which any of the possible single output-to-input FRFs (actuator-to-sensor, actuator-to-shaker, microphone-to-sensor or microphone-to-shaker) can be derived in such a way that they correspond accurately enough to the measured SISO FRFs. In this case *accurately enough* means that the eigenfrequencies of interest can be obviously recognized from the frequency responses obtained on the basis of the identified MIMO model. Through the iterative procedure it was found that the identified state-space model of the order n=85 fulfills such a condition. Lower model orders cannot provide pronounced eigenfrequencies of interest, while the higher model orders cause high computational effort without obvious improvement of the frequency response diagrams. Selected comparative FRFs are shown in the figures 9 and 10.

VI. Conclusion

The FEM approach and the system identification are shown to be useful tools for the modeling of smart acoustic structures. Depending on the available resources each of the suggested techniques can be used for a successful modeling.

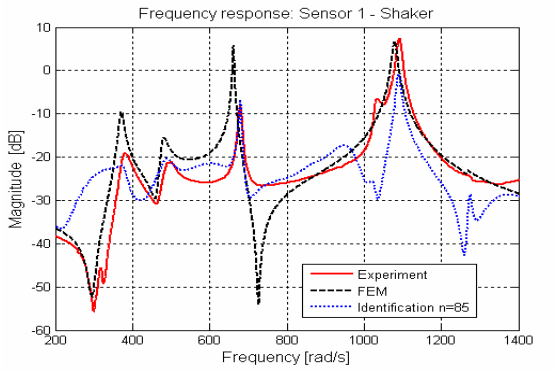

Fig. 9 FRFs *sensor 1 – shaker* determined experimentally, numerically and from the identified model (constellation 1)

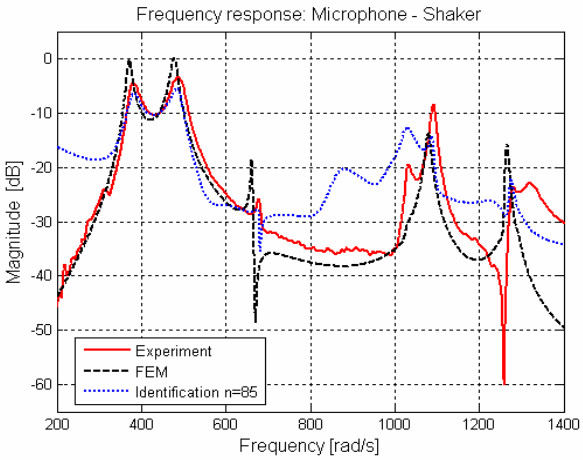

Fig. 10 FRFs *microphone – shaker* determined experimentally, numerically and from the identified model (constellation 1)

References

[1] J. Lefèvre, U. Gabbert, "Finite Element Simulation of Smart Structures for Active Vibration and Acoustic Control", *PAMM Proc. Appl. Math. Mech*. 3 (2003), pp. 296–297 DOI 10.1002/pamm.200310420.

[2] F. Laugwitz, J. Lefèvre, G. Schmidt, T. Nestorović, U. Gabbert, "Experimental and numerical investigation of a smart acoustic box", International Conference on Modal Analysis, Noise and Vibration Engineering ISMA2006 Leuven, Belgium, in CD-Proceedings of ISMA2006, editors P. Sas, M. de Munck, pp. 223–232.

[3] J. Lefèvre, U. Gabbert, "Finite Element Modelling of Vibro-Acoustic Systems for Active Noise Reduction", *Technische Mechanik* 25 (3–4), 2005, pp. 241–247.

[4] COSAR General Purpose Finite Element Package Manual 1992 FEMCOS mbH Magdeburg http://www.femcos.de

[5] P. Van Overschee, B. De Moor, *Subspace Identification for Linear Systems: Theory, Implementation, Applications*, Kluwer Academic Publishers, Boston 1996.

[6] M. Viberg, "Subspace-based methods for the identification of linear time-invariant systems", *Automatica* 31(12), 1995, pp. 1835–1851.

[7] T. Nestorović-Trajkov, H. Köppe, U. Gabbert, "Active Vibration Control Using Optimal LQ Tracking System with Additional Dynamics", *International Journal of Control*, vol. 78, no. 15, 15 October 2005, pp. 1182–1197.

[8] T. Nestorović, H. Köppe, U. Gabbert, "Subspace Identification for the model based controller design of a funnel-shaped structure", *Facta Universitatis, Series Mechanics, Automatic Control and Robotics*, vol. 4, no. 17, 2005, pp. 257–263.

[9] T. Nestorović-Trajkov, U. Gabbert, "Active control of a piezoelectric funnel-shaped structure based on subspace identification", *Structural Control and Health Monitoring*, vol. 13, no. 6, November/December 2006, pp. 1068–1079.

[10] T. Nestorović, *Controller Design for the Vibration Suppression of Smart Structures* (Ph.D. thesis), Fortschritt-Berichte VDI Reihe 8, Nr. 1071, Düsseldorf: VDI Verlag 2005.

[11] G. F. Franklin, J. D. Powell, M. L. Workman, *Digital Control of Dynamic Systems*, third edition, Addison-Wesley Longman, Inc., 1998.

[12] R. J. Vaccaro, *Digital Control: A State-Space Approach*, McGraw-Hill, Inc., 1995.

[13] T. Nestorović-Trajkov, U. Gabbert, „Overall virtual design and testing of adaptive mechatronic systems", Proceedings of the conference *Mechatronische Systeme – Entwurf, Anwendungen und Perspektiven*, organized in the frame of TEMPUS Project "Restrukturierung und Einführung der Mechatronik an den Universitäten in Serbien", September 27-28, 2006, Niš, Serbia (to be published).

[14] Matlab Help, Signal Processing Tooxbox, *n4sid*, http://www.mathworks.com/access/helpdesk/help/toolbox/ident/n4sid.html